Electronic Supplementary Material (ESI) for Journal of Materials Chemistry A.

Supporting Information

Dual-Source Evaporation of Silver Bismuth Iodide Films for Planar Junction Solar Cells

Maryam Khazaee,[ab] Kasra Sardashti,[a] Ching-Chang Chung,[c] Jon-Paul Sun,[ad] Hanhan Zhou,[c] Eric Bergmann,[d] Wiley A. Dunlap-Shohl,[a] Qiwei Han,[ae] Ian G. Hill,[d] Jacob L. Jones,[c] Doru C. Lupascu,[b] and David B. Mitzi*[ae]

[a] Department of Mechanical Engineering and Materials Science, Duke University, Durham, North Carolina 27708, United States
[b] Institute for Materials Science and Center for Nanointegration Duisburg-Essen (CENIDE), University of Duisburg-Essen, Universitätsstraße 15, 45141 Essen, Germany
[c] Department of Materials Science and Engineering, North Carolina State University, Raleigh, North Carolina 27695, United States
[d] Department of Physics and Atmospheric Science, Dalhousie University, Halifax, Nova Scotia B3H 3J5, Canada
[e] Department of Chemistry, Duke University, Durham, North Carolina 27708, United States
E-mail: david.mitzi@duke.edu

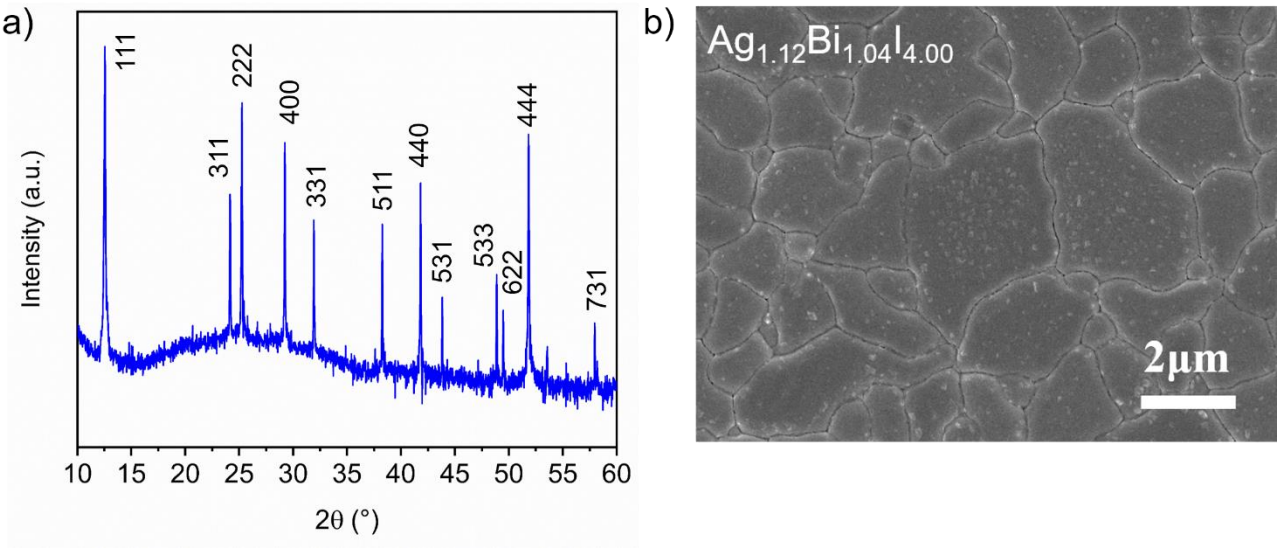

Fig. S1. a) Experimental XRD pattern of annealed/quenched thin film of Ag-Bi-I without excess of BiI_3 (180 °C for 15 min), which was deposited with *r* = 0.6 and b) SEM image of the thin film with the same noted composition.

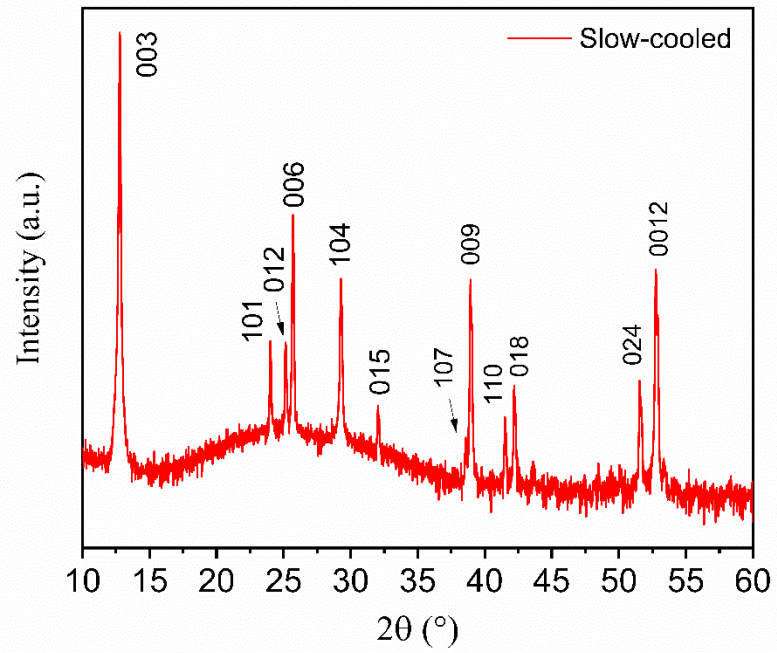

Fig. S2. Collected XRD pattern of annealed/slow-cooled thin film of Ag-Bi-I without excess of BiI_3 (180 °C for 15 min), which was deposited with *r* = 0.6.

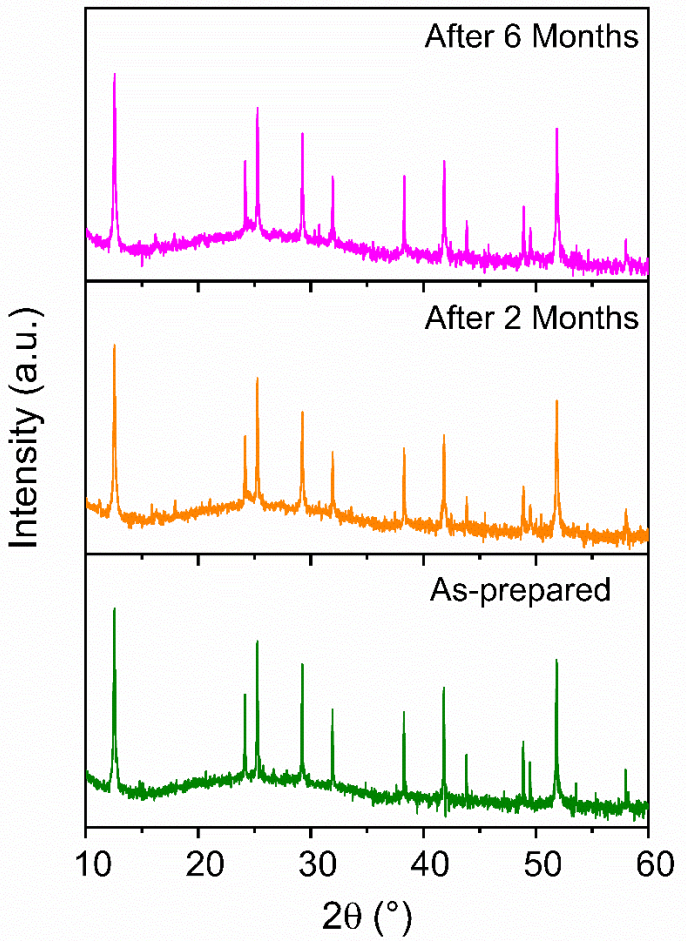

Fig. S3. Monitoring N_2 stability of the annealed (without an excess of BiI_3) *r* = 0.6 Ag-Bi-I film using XRD, demonstrating the stability of the cubic phase over at least 6 months.

Table S1 Crystallographic parameters and corresponding compositions of as-deposited and post-deposition annealed films of Ag-Bi-I achieved by Pawley refinement and SEM/EDX, respectively.

Ag-Bi-I Film	Composition (SEM/EDX)	Crystal System/space group	Unit Cell Parameters (Å)	Volume (Å^3)	Impurity	Fitting Parameters
0.2: As-deposited	$Ag_{0.49}Bi_{2.13}I_{7.00}$	Rhombohedral /$R\bar{3}m$	$a = b$ = 4.3502(3); c = 20.693(2)	339.14	BiI_3	Rp = 6.84 % wRp = 8.54 % GOF§ = 1.03
0.2: Annealed in N_2	$Ag_{0.72}Bi_{2.07}I_{7.00}$	Rhombohedral / $R\bar{3}m$	$a = b$ = 4.3479(4); c = 20.641(2)	337.92	BiI_3	Rp= 7.82 % wRp=9.81 % GOF= 1.28
		Cubic/ $Fd\bar{3}m$	$a = b = c$ = 12.1944(4)	1813.35		
0.6: As-deposited	$AgBi_{2.00}I_{7.00}$	Rhombohedral / $R\bar{3}m$	$a = b$ = 4.3546(1); c = 20.7430(3)	340.64		Rp = 6.84 % wRp = 8.94 % GOF = 1.35
0.6: Annealed under BiI_3	$Ag_{1.20}Bi_{1.85}I_{7.00}$	Cubic/ $Fd\bar{3}m$	$a = b = c$ = 12.2043(3)	1817.75		Rp= 7.97 % wRp=10.31 % GOF= 1.1
0.6: Annealed in N_2	$Ag_{1.12}Bi_{1.04}I_{4.00}$	Cubic/ $Fd\bar{3}m$	$a = b = c$ = 12.2079(2)	1819.39		Rp = 5.41 % wRp = 8.05 % GOF = 1.6
0.8: As-deposited	$Ag_{1.62}Bi_{1.06}I_{5.00}$	Rhombohedral / $R\bar{3}m$	$a = b$ = 4.3479(1); c = 20.8789(2)	341.82	AgI	Rp = 4.25 % wRp = 5.43 % GOF= 1.1
0.8: Annealed under BiI_3	$Ag_{1.85}Bi_{1.03}I_{5.00}$	Rhombohedral / $R\bar{3}m$	$a = b$= 4.3481(1); c = 20.8308(8)	341.06		Rp = 4.77 % wRp = 6.43 % GOF = 1.32
1.2: As-deposited	$Ag_{1.96}Bi_{0.95}I_{5.00}$	Rhombohedral / $R\bar{3}m$	$a = b$ = 4.3470(2); c = 20.8617(9)	341.40	AgI	Rp = 5.32 % wRp = 6.95 % GOF = 1.45
1.2: Annealed under BiI_3	$Ag_{1.91}Bi_{0.97}I_{5.00}$	Rhombohedral / $R\bar{3}m$	$a = b$ = 4.3510(2); c = 20.859(1)	341.98	AgI	Rp = 6.12 % wRp = 8.24 % GOF= 1.15

§ *GoF: Goodness of Fit*

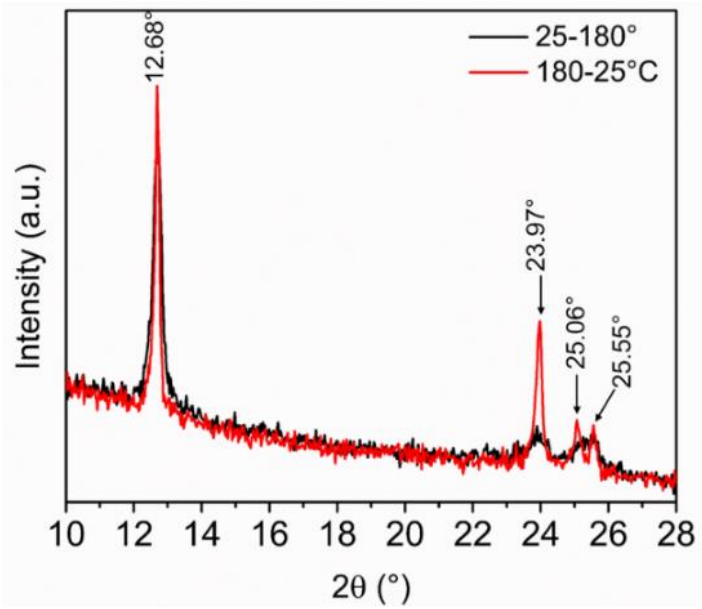

Fig. S4. Experimental XRD patterns of as-deposited thin film of Ag-Bi-I (black) with *r* = 0.8 at 25 °C and the annealed film from the TD XRD process (red) after cooling to 25 °C. Diffraction peaks at 12.68°, 23.97°, 25.06°, and 25.55° are assigned to 003, 101, 012, and 006 of rhombohedral Ag-Bi-I.

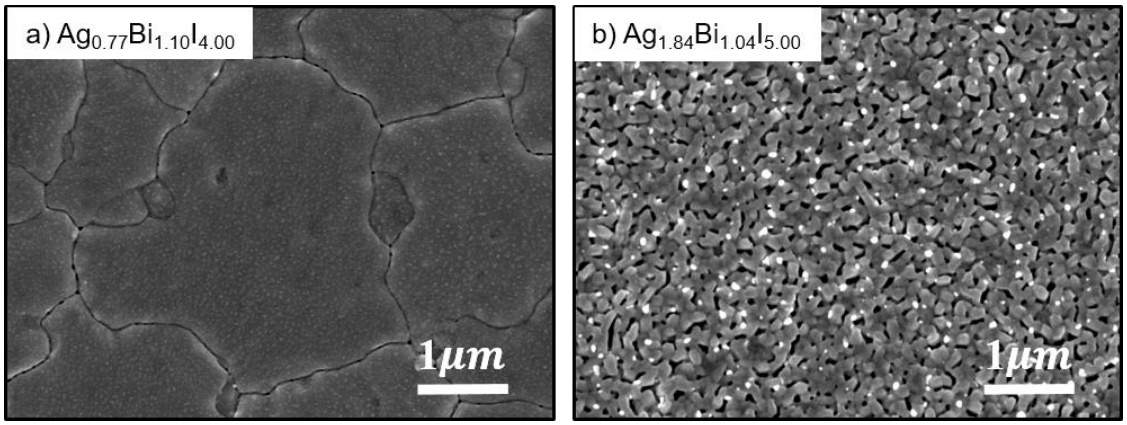

Fig. S5. SEM images of the annealed films from the TD XRD process with the associated compositions obtained from SEM/EDX; a) annealed film of *r* = 0.6 in N_2 (25°-180 °C, 180 °C for 1 h and cooled to 25 °C), b) annealed film of *r* = 0.8 in N_2 (25°-180 °C, 180 °C for 1 h and cooled to 25 °C).

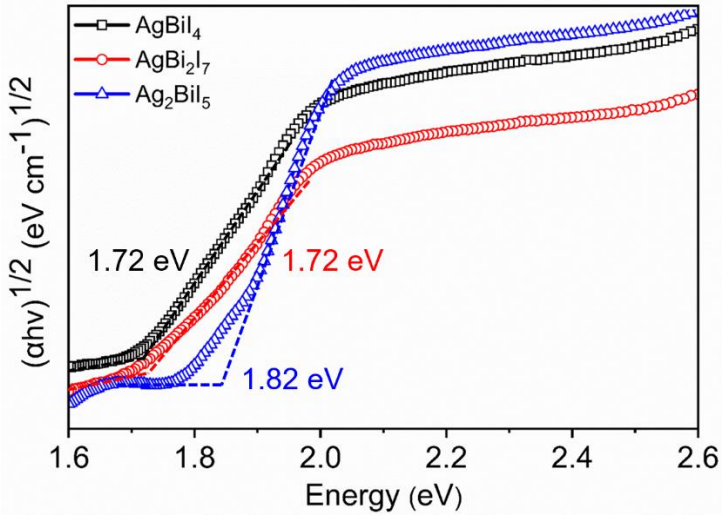

Fig. S6. Tauc plots showing indirect band gaps for $AgBi_2I_7$ (red), $AgBiI_4$ (black), and Ag_2BiI_5 (blue) films.

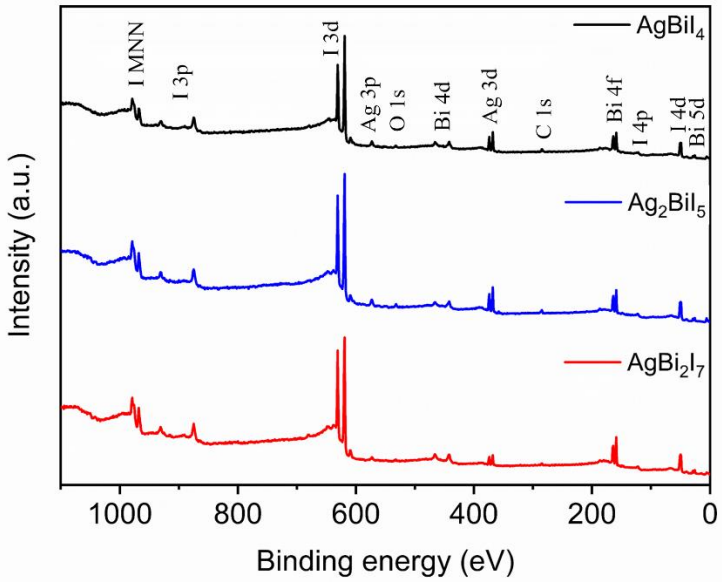

Fig. S7. XPS Al Kα survey scans of the as-loaded films of annealed r = 0.6 ($AgBi_2I_7$) and r = 0.8 (Ag_2BiI_5) at 180 °C under BiI_3 vapor and r = 0.6 ($AgBiI_4$) at 180 °C under N_2.

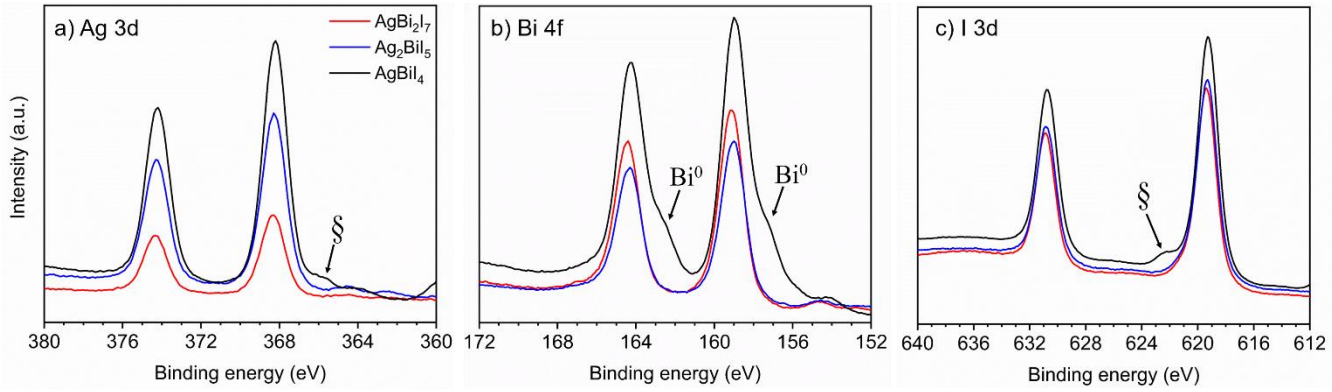

Fig. S8. Core level XPS (Al:$AgBi_2I_7$, Ag_2BiI_5; Mg:$AgBiI_4$) Kα spectra of a) Ag 3d, b) Bi 4f, and c) I 3d peaks for these films. Two small shoulders at ~162 eV and 157 eV in the Bi 4f spectrum for the $AgBiI_4$ film originate from metallic Bi (Bi^0). The small features marked with "§" are the Kα3 satellites of the 3d3/2 peaks, owing to a different excitation source (Mg vs. Al) used for core level spectra of $AgBiI_4$ ($\Delta E_{Mg\ K\alpha3\text{-}K\alpha1}$ = 8.5 eV, $\Delta E_{Al\ K\alpha3\text{-}K\alpha1}$ = 9.7 eV).

Table S2 Atomic ratios (%) derived from XPS for the annealed thin films of Ag-Bi-I (180 °C, 15 min) deposited with *r* = 0.6 and *r* = 0.8.

r = (AgI/BiI_3)	Ag (± 2)	Bi (± 1)	I (± 3)	Composition
0.6[a]	9	17	74	$AgBi_{1.9}I_{8.2}$
0.6[b]	21	22	57	$AgBiI_{2.7}$
0.8[a]	18	13	69	$Ag_{2.0}Bi_{1.1}I_{5.3}$

[a] *annealed under BiI_3;* [b] *annealed under N_2*

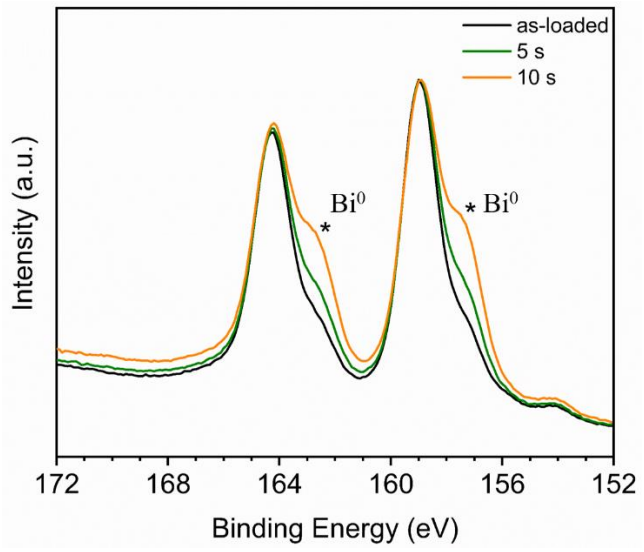

Fig. S9. Close-up Mg Kα scans of Bi4f peaks for as-loaded, 5 s, and 10 s sputtered thin film of $AgBiI_4$. Two small shoulders at ~162 eV and 157 eV originate from metallic Bi (Bi^0).

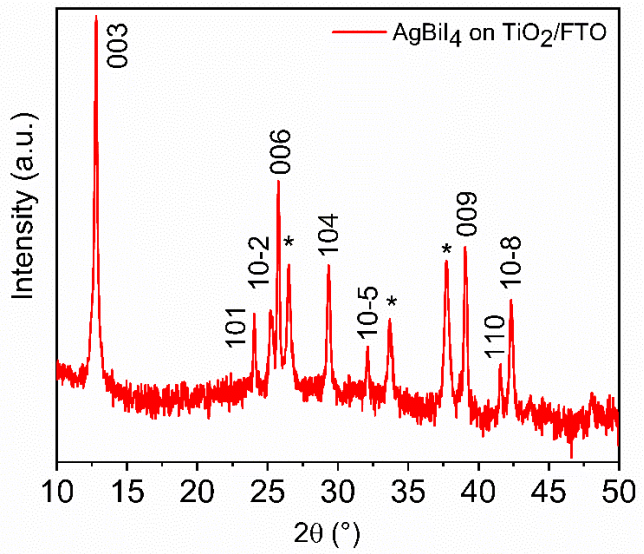

Fig. S10. Experimental XRD pattern of annealed/slow-cooled thin film of Ag-Bi-I without excess of BiI_3, which was deposited with r = 0.6 on TiO_2/FTO. The labeled peaks with "*" originate from FTO.